Supporting Information

Well-defined S-g-C_3N_4/Cu-NiS heterojunction interface towards enhanced spatial charge separation with excellent photocatalytic ability: synergetic effect, kinetics, antibacterial activity, and mechanism insights

Haya A. Abubshait[1‡], Shahid Iqbal[2*‡], Samar A. Abubshait[3], Mohammed T. Alotaibi[4], Norah Alwadai[5], Nada Alfryyan[5], Hashem O. Alsaab[6], Nasser S. Awwad[7], Hala A. Ibrahium[7,8]

[1]*Basic Sciences Department, Deanship of Preparatory Year and Supporting Studies, Imam Abdulrahman Bin Faisal University, P.O. Box 1982, Dammam 31441, Saudi Arabia.*

[2]*Department of Chemistry, School of Natural Sciences (SNS), National University of Science and Technology (NUST), H-12, Islamabad, 46000, Pakistan.*

[3]*Department of Chemistry, College of Science, Imam Abdulrahman bin Faisal University, P.O. Box 1982, Dammam 31441, Saudi Arabia.*

[4]*Department of Chemistry, Turabah University College, Taif University, P.O. Box 11099, Taif 21944, Saudi Arabia.*

[5]*Department of Physics, College of Sciences, Princess Nourah bint Abdulrahman University, P.O. Box 84428, Riyadh 11671, Saudi Arabia.*

[6]*Department of Pharmaceutics and Pharmaceutical Technology, Taif University, P.O. Box 11099, Taif 21944, Saudi Arabia.*

[7]*Research Center for Advanced Materials Science (RCAMS), King Khalid University, P.O. Box 9004, Abha, 61413, Saudi Arabia.*

[8]*Department of Semi Pilot Plant, Nuclear Materials Authority, P.O. Box 530, El Maadi, Egypt.*

To whom corresponding should be addressed

shahidiqbal.chem@sns.nust.edu.pk (Shahid Iqbal)

‡ The authors have equal contribution

2.6.1. Material characterization

The microstructure and morphology of the fabricated materials were analyzed by TEM (JEM-2100) and SEM (TESCAN Vega 3). The crystal structure was studied by XRD (PANalytical X'Pert) and EDX was recorded with SEM (Hitachi S4800). FTIR spectra were analyzed by Brucker Tensor 27. XPS tests were carried on VG Scientific spectrometer (ESCA Lab220i-XL) outfitted with Al Kα signals in twin anode at 14 kV × 16 Ma, standardized via the control carbon (C 1s

284.6 eV). Photoluminescence (PL) analysis was checked by using a PL-FS-2500 (Japan) fluorescence spectrometer. The photocatalytic and optical measurements were carried out by (UV-3600, Shimadzu) a UV-vis spectrometer. The Brunauer-Emmett-Teller (BET) surface area was examined (Micromeritics ASAP 2020 instrument) through N_2 adsorption in a computerized gas-sorption machine. Transient photocurrent response tests were conducted on a standard three-electrode system (CHI 602 Electrochemical Workstation) at 25 ^oC with the Pt wire as the counter electrode, photocatalyst-coated FTO as the working electrode and Ag/AgCl as a reference electrode (Shanghai Chenhua Instrument Co. Ltd, Shanghai, China). The EIS was assessed at -0.6 V (vs. Ag/AgCl) from 10^5 to 0.1 Hz with a signal amplitude of 20 mV. The ESR signals were collected on a JES FA200, JEOL Co. spectrometer with the 5,5-dimethyl-1-pyrroline-N-oxide (DMPO) solvent.

2.6.2. Photocatalytic ability

Assessments on the photocatalytic ability were conducted under visible light ($\lambda \geq 420$) source via exploitation of a 350 W Xe lamp at 25 oC. In the MB degradation testing, 100 mg of each constructed material was disseminated in 100 mL of dye solution (10 mg L-1). Each catalyst dispersion was retained under dark for 30 min with continuous strong stirring magnetically to equilibrize the photocatalytic system and then exposed to visible light to induce photocatalysis. At systematic intervals, 4 mL of sample aliquots were taken out and centrifuged at 6000 rpm for 5 minutes. Then absorption characteristics of each centrifuged aliquot was measured (JASCO-V-770) by a UV-visible spectrophotometer. The chemical stability of designed materials was explored and the results of up to 7 cycles are presented in Fig. 8a.

2.6.3. Antimicrobial activity

The antibacterial activities of the S-g-C_3N_4, NiS NRs, Cu-NiS NRs and Cu-NiS/S-g-C_3N_4 binary NCs compared to Gram-positive and Gram-negative bacterial varieties were estimated by the agar well diffusion method. B. subtilis, S. aureus, S. salivarius (gram-positive bacteria) and E. coli as gram-negative bacterium strains were bought from Sigma-Aldrich. Ciprofloxacin (0.5 mg/mL) was employed as positive control and double DI water was used as the negative control. Ultrasonically S-g-C_3N_4, NiS NRs, Cu-NiS NRs and Cu-NiS/S-g-C_3N_4 NCs suspensions were prepared water at a concentration of 0.5 mg/mL.

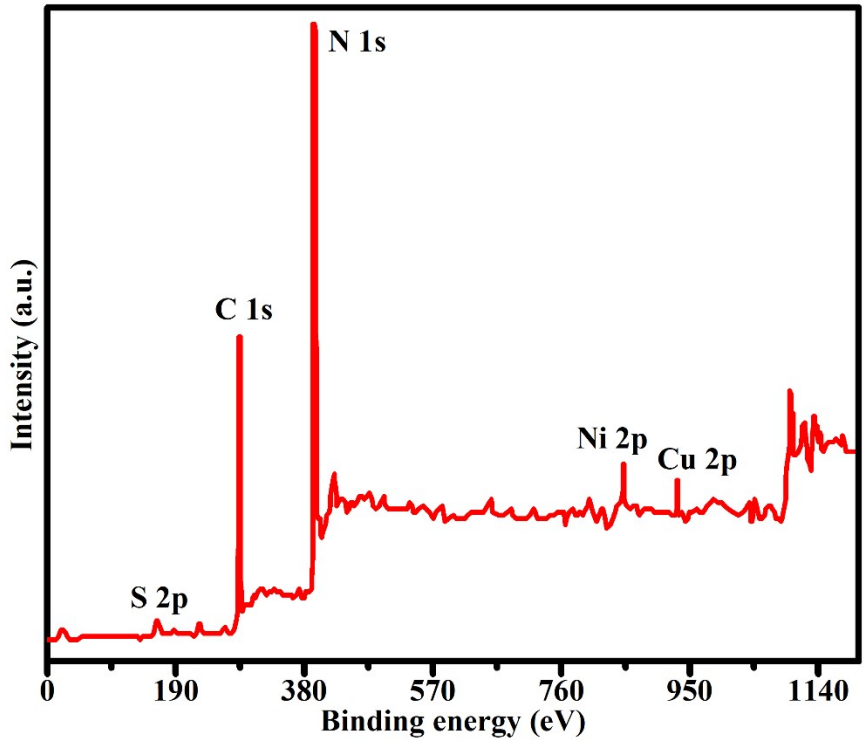

Fig. S1. XPS survey spectrum of 22% 2D/1D SCN/CNS heterojunction.

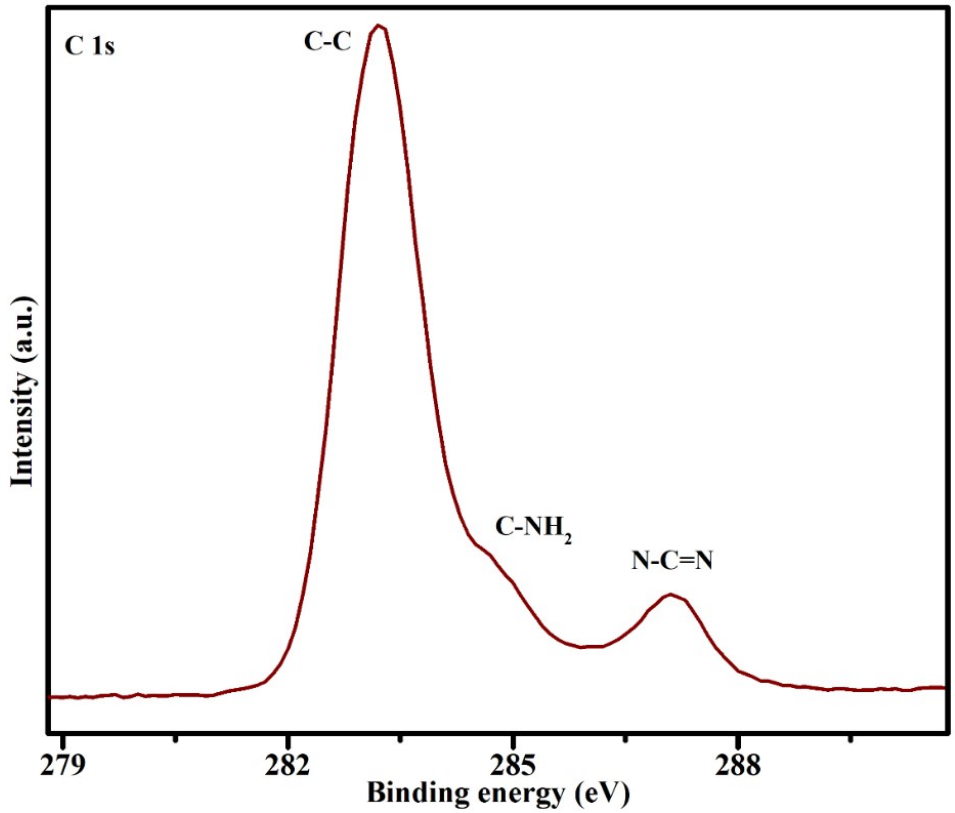

Fig. S2. High-resolution XPS C 1s spectra of 18% 1D/2D Cu-NiS/S-g-C_3N_4 heterojunction.

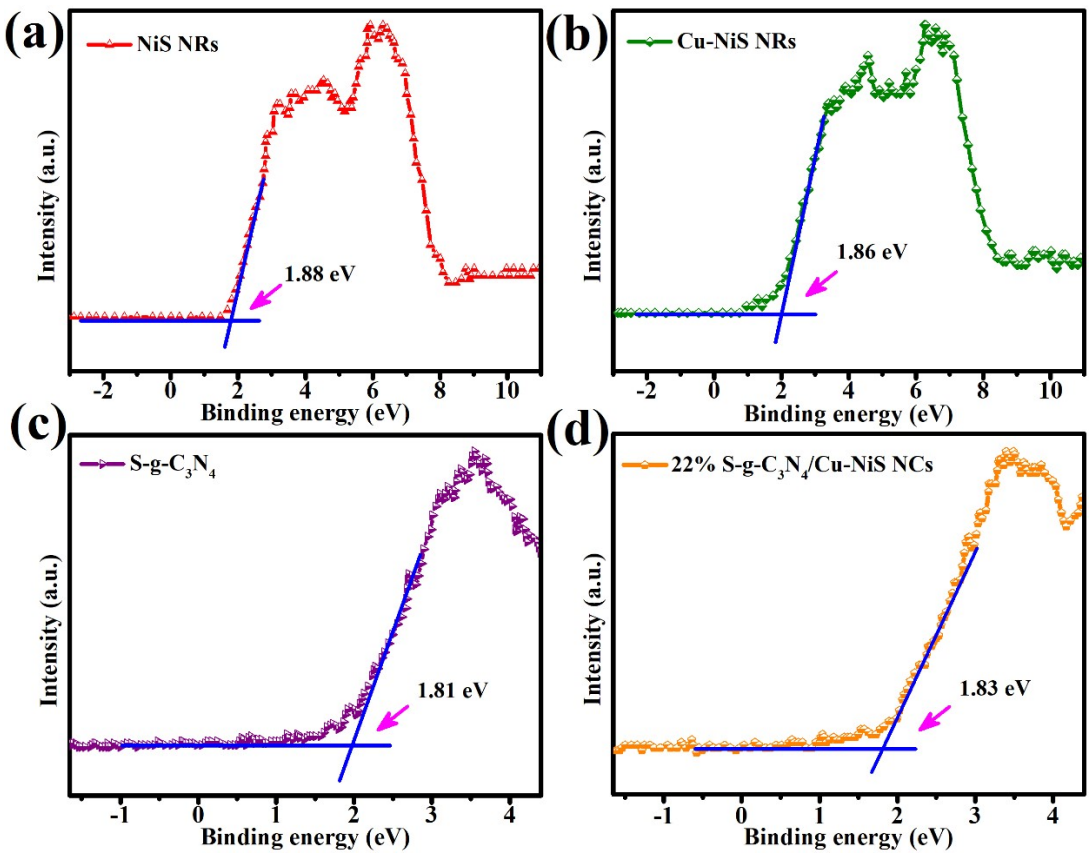

Fig. S3. Valence-band XPS spectra of (a) NiS, (b) 7% Cu-NiS, (c) SCN and (d) 22% SCN/7CNS NCs.

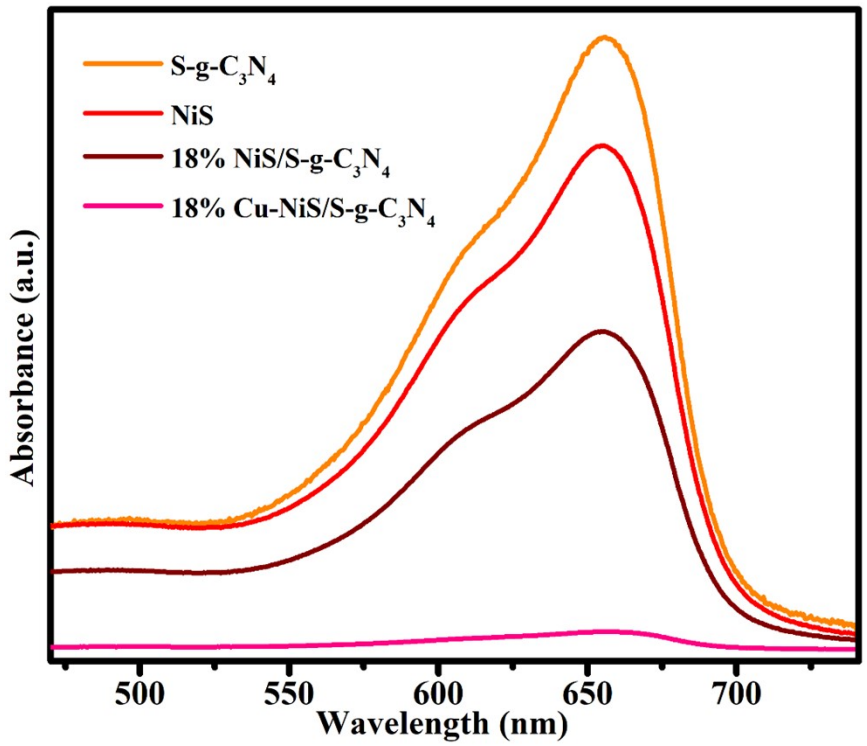

Fig. S4. The evaluation of MB photodegradation under visible-light illumination after 36 min for pristine S-g-C_3N_4, undoped NiS NRs, 18% NiS/S-g-C_3N_4 heterostructure and 18% 1D/2D Cu-NiS/S-g-C_3N_4 binary NCs.

Table S1. Bactericidal Efficiency of NiS NRs, Cu-NiS NRs, S-g-C_3N_4 and 22% 2D/1D SCN/CNS NCs.

Antimicrobial agent	Escherichia Coli (mm)	Bacillus subtilis (mm)	Streptococcus salivarius (mm)	Staphylococcus aureus (mm)
Negative control	00	00	00	00
Positive control	17	18	21	16
NiS NRs	4.5	2.5	3.5	2.5
Cu-NiS NRs	6.5	4.5	6.5	5.5
S-g-C_3N_4	09	07	10	09
Cu-NiS/S-g-C_3N_4 NCs	18	16	20	17

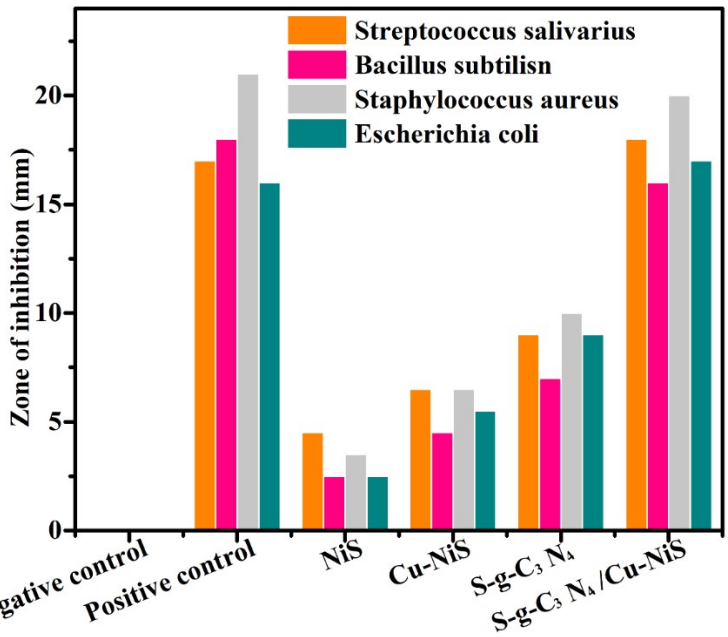

Fig. S5. Zone of inhibition (mm) of NiS NRs, Cu-NiS NRs, S-g-C_3N_4, and 22% 2D/1D SCN/CNS NCs against Staphylococcus aureus, Streptococcus salivarius, Bacillus subtilis and Escherichia Coli.